

Cite this: *J. Mater. Chem. C*, 2025, 13, 4104

# Dual-channel regulation of a single white-light-emitting compound and its application in time-dependent information encryption†

Yuehua Liang,<sup>a</sup> Jiuzhi Wei,<sup>a</sup> Juan Zhang,<sup>a</sup> Tingting Zhang,<sup>a</sup> Caiyuan Guo,<sup>a</sup> Yanyan Li,<sup>a</sup> Xinxian Ma,<sup>a</sup> \*<sup>a</sup> Minghua Liu \*<sup>b</sup> and Yun Yan \*<sup>a,c</sup>

Dual-channel regulation of single-molecular white-light fluorescence is proposed. It was found that a newly synthesized bis-phenanthroimidazole (PI) compound could show white-light emission based on acid or base induction through multiple non-covalent interactions. Specifically, the addition of H<sup>+</sup> or OH<sup>-</sup> to a dimethyl sulfoxide solution of PI compound causes an emission transition from blue light to white light, owing to protonation of the PI compound. The mixing of the different intermediate species can emit fluorescence of various colors, and approach white-light emission. Further, a multipurpose gel composed of polyvinyl alcohol and PI is prepared, which can serve as an information-writing material. It is found that the film shows no color at the beginning when the information is written. However, when water is evaporated onto the film, the information appears gradually. After the film is dried, the information can be erased again. Thus, a time-dependent and water-vapor-driven information-encryption system is developed, which can provide new insights into the design and application of information-encryption materials.

Received 11th November 2024,  
Accepted 24th December 2024

DOI: 10.1039/d4tc04771k

rsc.li/materials-c

## 1. Introduction

Organic fluorescent white-light-emitting materials are a new type of flourishing functional luminescent material. Given their low cost, light weight, ease of synthesis, and ability to form ultrathin films, these materials have broad application prospects in temperature monitoring, sensing, biological imaging, and information technology fields.<sup>1,2</sup> Compared with inorganic white-light-emitting materials, organic counterparts show better adjustability, more diversity in molecular design, lower manufacturing costs and lower toxicity.<sup>3</sup> There are two methods to develop white-light-emitting materials. A general one is to mix different fluorescent molecules. The essence of this strategy is based on color complementation to generate white light (400–700 nm). The most commonly used method for

white-light generation is mixing of the three primary colors (blue, green, and red). Further, based on the concept of the complementary colors of white light, mixing one of the three primary colors with yellow, purple, or blue can also produce white light. However, given the considerable differences in the emission brightness, wavelength range, and stability of sources emitting different colored lights,<sup>4,5</sup> white light produced by mixing dyes exhibits poor purity and stability. This creates a challenge to develop single-molecule-based white-light emission with unique advantages in material preparation and application.<sup>6–10</sup> To achieve white-light emission from single molecules, mixed solvents with different polarities are usually adopted, which causes the molecules to exhibit different conformations or undergo an excited-state proton transfer process to simultaneously emit light with two complementary fluorescence channels. For example, Maity *et al.* prepared a single molecule that can emit blue–green–white–yellow colors by adjusting the water content in a tetrahydrofuran–water mixed solution, based on excited-state intermolecular proton transfer coupled with an aggregation-induced emission enhancement process.<sup>11</sup> Alonso *et al.* selectively protonated the amino group by adding a specific amount of acid, causing 1,3-disubstituted indolizine compounds to emit red–white–blue colored light.<sup>12</sup> However, currently reported organic white-light-emitting materials are based mainly on multichannel-emission-modulation compounds processed using dual-solvent systems. There is a

<sup>a</sup> Ningxia Key Laboratory of Green Catalytic Materials and Technology, College of Chemistry and Chemical Engineering, Ningxia Normal University, Guyuan 756099, China. E-mail: maxinxian@163.com

<sup>b</sup> CAS Key Laboratory of Colloid, Interface and Chemical Thermodynamics, Institute of Chemistry, Chinese Academy of Sciences, Beijing, P. R. China. E-mail: liumh@iccas.ac.cn

<sup>c</sup> Beijing National Laboratory for Molecular Sciences (BNLMS), College of Chemistry and Molecular Engineering, Peking University, Beijing 100871, China. E-mail: cqhuar@126.com, yunyan@pku.edu.cn

† Electronic supplementary information (ESI) available. See DOI: <https://doi.org/10.1039/d4tc04771k>

strong need to develop a white-light emission system based on a single molecule in a single solvent.

In this article, we modify the pyrrole nitrogen on phenanthroimidazole, which results in a significant twisting angle between the functional group on the pyrrole nitrogen and the phenanthroimidazole plane, to almost perpendicular. This will to some extent inhibit intermolecular aggregation, block intramolecular charge transfer, and ensure its blue emission. We have designed a derivative of bis-phenanthroimidazole (PI) imidazole based on this theory (Scheme S1, ESI<sup>†</sup>). It was found that the PI molecule can be affected by acids or alkalis in DMSO solution, which causes its protonation and different types of stacking due to electrostatic and p-p interactions.<sup>13–18</sup> This phenomenon exposes the blue and yellow dual-fluorescence channels of the PI molecule. When the H<sup>+</sup> or OH<sup>-</sup> concentration reaches a certain value in the DMSO solution, the PI molecule can precisely emit white light. We further used polyvinyl alcohol (PVA) as a carrier to develop a white-light-emitting PVA/(PI + 100 eq. H<sup>+</sup>) gel. In addition, we have developed an information-encryption material based on a time-dependent fluorescent hydrogel (Fig. 1). Previous studies have shown that the fluorescence emitted by a molecule can be controlled not only by the chemical reaction of the fluorophore, but also by the dynamic network structure of the polymer.<sup>19,20</sup> For example, protonation of fluorescent groups can be controlled by adding two easily decomposable components, urea and hydrochloric acid, to the polymer, so that the fluorescence emitted by the fluorescent group is influenced by time. Therefore, we introduced PI into the

pH-responsive hydrogel network to develop white-light hydrogels. The degree of molecular protonation can be controlled by adjusting the content of protons in the hydrogel network, to achieve control over fluorescence color. On this basis, an information-encryption material with self-erasure has been developed. The information can be encoded by introducing water into the gel and automatically deleted over time without complicated encryption and decryption processes.

## 2. Experimental section

For the synthesis of PI, see Scheme S1 (ESI<sup>†</sup>).

### 2.1. Materials and general methods

PVA (polymerization degree = 1799, 98–99% alcoholysis) was purchased from Energy Chemical. Ethyl chloroacetate, *N,N*-dimethylformamide (DMF), methylbenzene, potassium carbonate, methanol, ethyl alcohol, potassium iodide, acetic acid, ammonium acetate, phenanthrene-9,10-dione, ethylene glycol, 1,4-dioxane, 4,4'-biph-enydicarbaldehyde, DMSO, metal salts, pyridine, acetonitrile, sulfuric acid, ethyl acetate, acetone, tetrahydrofuran, dichloromethane, and sodium hydroxide were procured from Sinopharm Chemical Reagent Co., Ltd. All the compounds were used directly without further purification, and distilled water was used for all experiments.

Proton nuclear magnetic resonance (<sup>1</sup>H NMR; 400 MHz) and <sup>13</sup>C NMR (101 MHz) spectroscopic analyses were performed

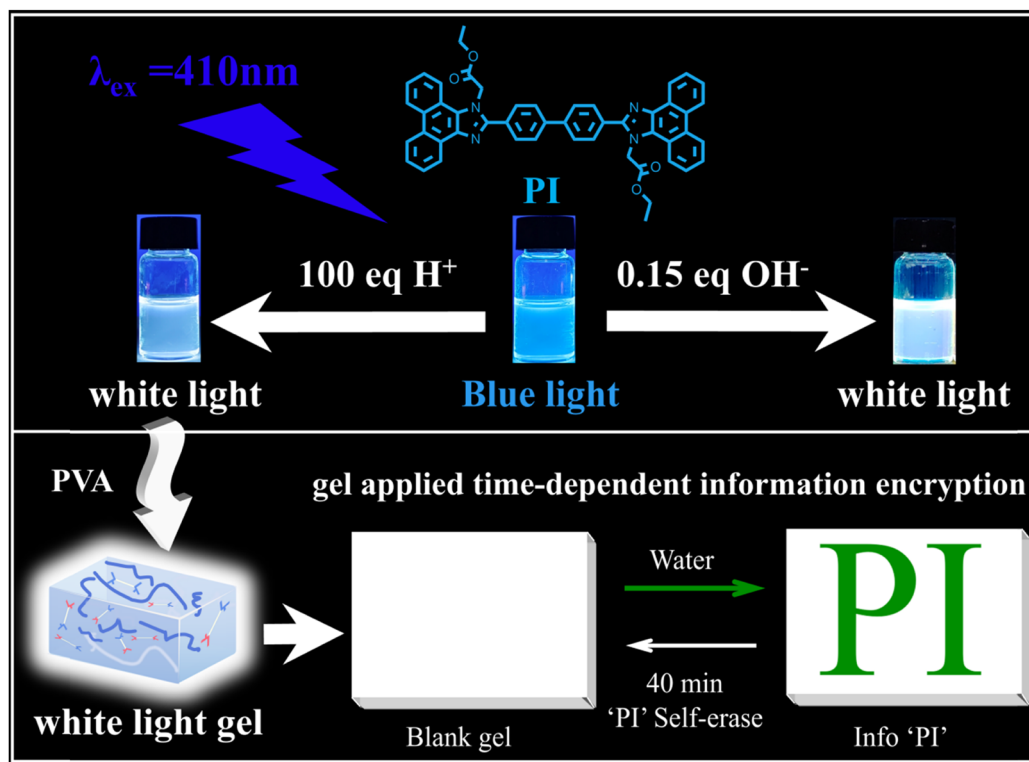


Fig. 1 Schematic diagram of dual-channel regulation of a white-light-emitting bis-phenanthroimidazole compound and its application in time-dependent information encryption.

using a 400-MHz Bruker spectrometer. A Shimadzu RF-6000 fluorescence spectrophotometer was used to obtain the fluorescence spectra. Mass spectrometry was determined using an Autoflex Speed TOF/TOF. Fourier transform infrared (FT-IR) spectra of the samples were obtained using an IR spectrophotometer (Thermo Scientific Nicolet iS5) in a wavenumber range of 400–4000  $\text{cm}^{-1}$ . The quantum yields (QYs) were determined using an Edinburgh FLS1000 instrument. A Shimadzu UV-1750 spectrometer was used to record the ultraviolet-visible (UV-vis) absorption spectra of the samples. The fluorescence lifetimes were recorded on a time-correlated single-photon counting spectrometer (Edinburgh FLS1000). Quantum chemistry calculations were performed at the PBE0/6-311G\* level of theory based on time-dependent density functional theory (TD-DFT) using Gaussian 09 software.<sup>21,22</sup>

## 2.2. Synthesis of compounds. synthesis of compound 1

As shown in Scheme S1 (ESI<sup>†</sup>), 9,10-phenanthraquinone (4.00 g, 19.21 mmol), ammonium acetate (15.00 g, 0.19 mol), and biphenyl dialdehyde (2.02 g, 9.61 mmol) were dissolved in 60 mL of acetic acid, and the mixture was stirred at 130 °C for 8 h. Following cooling to room temperature, the product was diluted with water and washed thrice *via* filtration using water. Following vacuum drying of the product, a yellow powder was obtained (5.29 g, yield: 93.90%). <sup>1</sup>H NMR (400 MHz, DMSO-*d*<sub>6</sub>, Fig. S1, ESI<sup>†</sup>)  $\delta$  13.58 (s, 2H), 8.93–8.86 (m, 4H), 8.62 (ddd, *J* = 14.9, 8.0, 1.4 Hz, 4H), 8.51–8.45 (m, 4H), 8.13–8.07 (m, 4H), 7.81–7.74 (m, 4H), 7.70–7.64 (m, 4H). <sup>13</sup>C NMR (101 MHz, DMSO-*d*<sub>6</sub>, Fig. S2, ESI<sup>†</sup>)  $\delta$  149.41, 140.15, 130.29, 128.11, 127.60, 127.52, 127.22, 125.73, 124.41, 122.51.

## 2.3. Synthesis of PI

As shown in Scheme S1 (ESI<sup>†</sup>), compound 1 (2.32 g, 3.96 mmol) was dissolved in DMF (40 mL), followed by the addition of potassium carbonate (1.50 g, 10.85 mmol), potassium iodide (0.2 g, 1.20 mmol), and ethyl chloroacetate (2.50 g, 20.40 mmol). The resulting mixture was stirred at 110 °C for 10 h. The product was diluted with water, filtered, and washed five times using water. Following vacuum drying of the product, a light-yellow solid was obtained (2.75 g, yield: 91.67%). <sup>1</sup>H NMR (400 MHz, DMSO-*d*<sub>6</sub>, Fig. S3, ESI<sup>†</sup>)  $\delta$  9.02 (dd, *J* = 8.6, 1.4 Hz, 2H), 8.91 (d, *J* = 8.4 Hz, 2H), 8.66 (dd, *J* = 8.0, 1.5 Hz, 2H), 8.19 (dd, *J* = 8.2, 1.5 Hz, 2H), 8.12–8.05 (m, 4H), 7.94–7.89 (m, 4H), 7.77–7.68 (m, 8H), 5.63 (s, 4H), 4.30 (q, *J* = 7.1 Hz, 4H), 1.25 (t, *J* = 7.1 Hz, 6H). <sup>13</sup>C NMR (the solubility of PI in a deuterated DMSO solvent was extremely low). High-resolution mass spectrometry (ESI, <sup>†</sup> Fig. S4): *m/z* calcd for C<sub>50</sub>H<sub>38</sub>O<sub>4</sub>N<sub>4</sub> [M + H]<sup>+</sup>: 759.890; found: 759.695.

## 2.4. Synthesis of PVA/(PI + 100 eq. H<sup>+</sup>) gel

PVA (2.2 g, 0.05 mol, alcohol degree >99.5 mol%) was dissolved in 10 mL of DMSO solution with a concentration of  $1 \times 10^{-3}$  mol L<sup>-1</sup> PI, and then 100  $\mu$ L of concentrated sulfuric acid was added. The mixture was heated and stirred at 100 °C for 6 h. The solution was poured into a culture dish, which was placed in a refrigerator and refrigerated at -10 °C for 12 h.

Then the solution was taken out to thaw to obtain a white fluorescent gel.

# 3. Results and discussion

## 3.1. Single-molecule white emission triggered by protons

By studying the fluorescence emission spectra of PI in polar and non-polar solvents (Fig. 2), we found that PI exhibits deep blue luminescence in non-polar solvents and sky blue luminescence in polar solvents (Fig. S5, ESI<sup>†</sup>). At the same time, the solubility of PI in polar solvents is better than in non-polar solvents, but the maximum solubility that PI can achieve in polar solvents is only about  $1 \times 10^{-3}$  mol L<sup>-1</sup>. Therefore, we will use DMSO, the solvent with the highest polarity, as the solvent for PI in the following tests. Subsequently, we calculated the HOMO and LUMO orbitals of PI and compared the calculated fluorescence emission spectra of PI with the actual fluorescence emission spectra of PI in DMSO solution. We found that the difference between the two was not significant. The optimal fluorescence emission spectrum peak calculated for PI is 488 nm, converted to an absolute energy value of 2.54 eV. The experimentally measured optimal fluorescence emission spectrum peak is 458 nm, converted to an absolute energy value of 2.71 eV, with a difference of 0.17 eV between the two, within a reasonable range of calculation error of  $\pm 0.3$  eV. Furthermore, we measured the optimal emission and absorption spectra of PI, and based on these results, we fixed the wavelength of PI excitation at 410 nm for subsequent testing. It is worth mentioning that PI shows an AIE effect (Fig. 2f, g and Fig. S6, ESI<sup>†</sup>).

Interestingly, after conducting cation and anion recognition tests for a DMSO solution of PI, we observed that acidic and alkaline environments caused the fluorescence emission of PI to exhibit new peaks (Fig. S7, ESI<sup>†</sup>). Notably, within a certain concentration range, the addition of acids and bases caused white-light emission from the DMSO solution of PI. To gain in-depth insights into the effects of acids and bases on the DMSO solution of PI, we conducted various tests using acids and bases separately. Fig. 3a and b show that with increasing hydrogen concentration, the blue-light-emitting component of the DMSO solution of PI gradually decreased while the red-light-emitting component gradually increased. At the same time, the absorption spectrum of PI shows that the absorption peak of PI decreases with an increase of hydrogen ion concentration. In addition, the DMSO solution of PI also changed emission from blue to white light. As shown in Fig. 3c–e, when the hydrogen-ion concentration was between 20 and 200 eq., the DMSO solution of PI emitted white light. However, at a hydrogen-ion concentration of 100 eq., the white light emitted by the DMSO solution of PI (0.30, 0.35) was closer to the pure white-light spot (0.33, 0.33).

Further, we used <sup>1</sup>H NMR to investigate the effect of H<sup>+</sup> on PI in DMSO solvent. The gradual addition of sulfuric acid solution to the DMSO-*d*<sub>6</sub> solution of PI resulted in the progressive deshielding of all signals, except those of the methylene and ester groups. After adding 100 eq. of H<sup>+</sup>, the signal

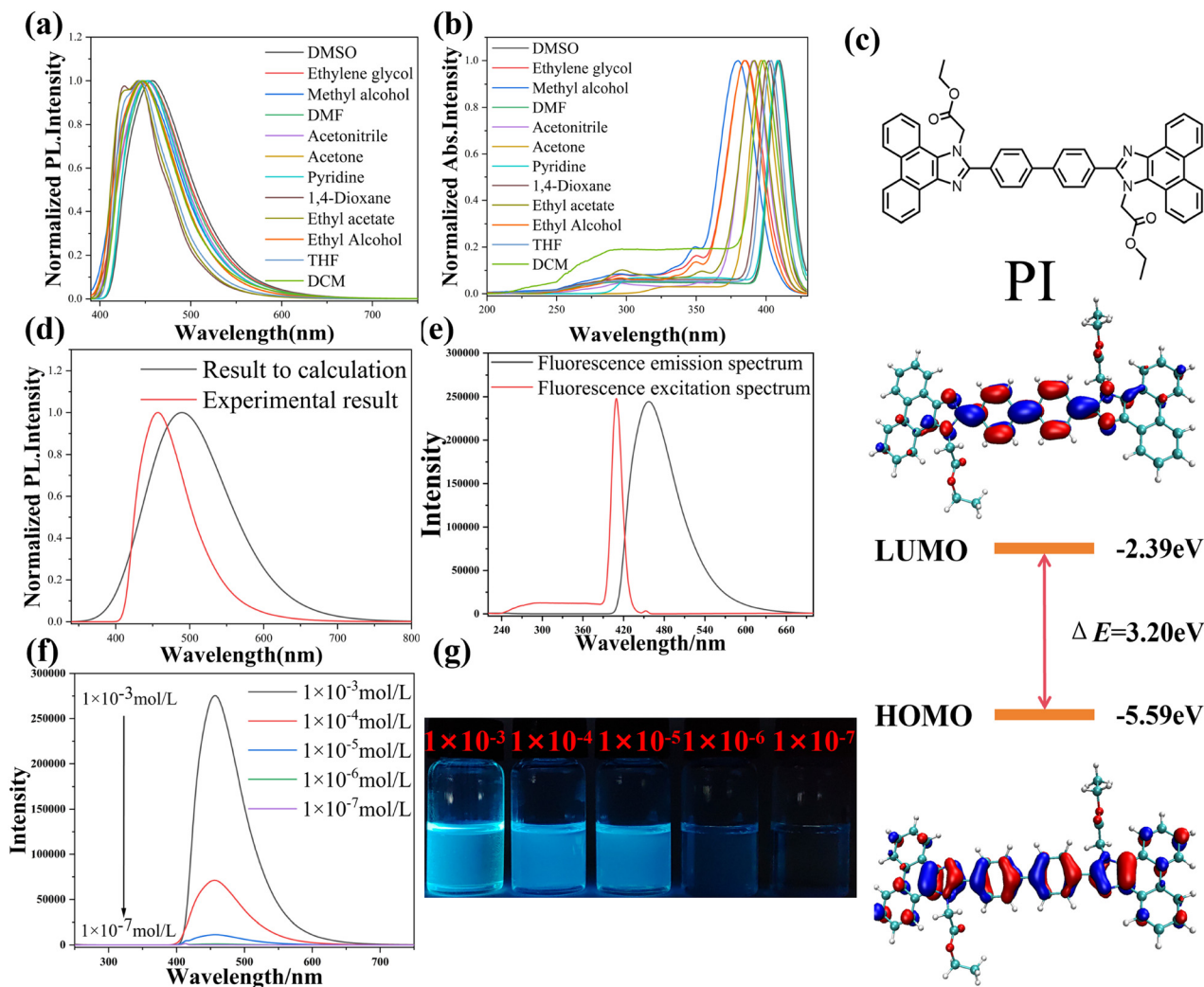


**Fig. 2** (a) Normalized emission spectra of PI in different solvents. (b) Normalized absorption spectra of PI in different solvents. (c) Representation of HOMO–LUMO and energy gap in PI (structural optimization and excited state calculation at the PBE0/6-311G\* level). (d) Comparison of the fluorescence emission spectrum of PI calculated using Gaussian 09 software and the actual fluorescence emission spectrum of PI in DMSO solution. (e) The optimal fluorescence emission spectrum and fluorescence absorption spectrum of PI in DMSO solution. (f) Fluorescence emission spectroscopy of  $1 \times 10^{-3}$ ,  $1 \times 10^{-4}$ ,  $1 \times 10^{-5}$ ,  $1 \times 10^{-6}$ , and  $1 \times 10^{-7}$  mol L<sup>-1</sup> PI in DMSO solution. (g) Images of  $1 \times 10^{-3}$ ,  $1 \times 10^{-4}$ ,  $1 \times 10^{-5}$ ,  $1 \times 10^{-6}$ , and  $1 \times 10^{-7}$  mol L<sup>-1</sup> PI in DMSO solution under UV light from left to right.

corresponding to the aromatic-ring hydrogen of PI was considerably deshielded (Fig. S8 and S9, ESI<sup>†</sup>). Based on this result, we speculate that as H<sup>+</sup> are gradually added to the DMSO solution of PI, PI undergoes protonation, and when 100 eq. of H<sup>+</sup> are added, the free PI in the solution is almost completely transformed into PI with different degrees of protonation. The protonated PI exhibits varying degrees of red shift in its luminescence, ultimately leading to the emission of white light.

Subsequently, FT-IR spectroscopy was used to elucidate the interactions between the aromatic ring of PI and H<sup>+</sup> after the addition of 100 eq. of H<sup>+</sup>. The out-of-plane bending vibration of the C–H bond on the aromatic ring of pure PI in DMSO solution was observed at 956 cm<sup>-1</sup> (Fig. S10, ESI<sup>†</sup>). However, after adding 100 eq. of H<sup>+</sup>, the C–H out-of-plane bending vibration of PI in DMSO solution was blue shifted by 31 cm<sup>-1</sup> (PI +

100 eq. H<sup>+</sup>: 987 cm<sup>-1</sup>), confirming the existence of interaction forces between PI and H<sup>+</sup>.

To confirm the interaction forces between PI molecules and H<sup>+</sup> or OH<sup>-</sup>, we used DFT to optimize the molecular structure of PI and plotted its ESP distribution. The pyrrole nitrogen atom on the imidazole ring of PI and lone-pair electrons provided by its adjacent carbonyl group formed an electron-rich region (ESP: -20 kcal mol<sup>-1</sup>), which provided a basis for cation-π interactions between PI and H<sup>+</sup> (Fig. 4a). Meanwhile, there was an electron-poor region (ESP: 20 kcal mol<sup>-1</sup>) between the antibonding orbitals of pyrrole nitrogen atoms on the imidazole ring of PI and adjacent carbonyl groups, which provided a basis for the interaction between PI and OH<sup>-</sup>.

TD-DFT was used to calculate the fluorescence emission energy of PI in DMSO solution, and the protonated compound of PI was used to simulate the structure formed by cation-π

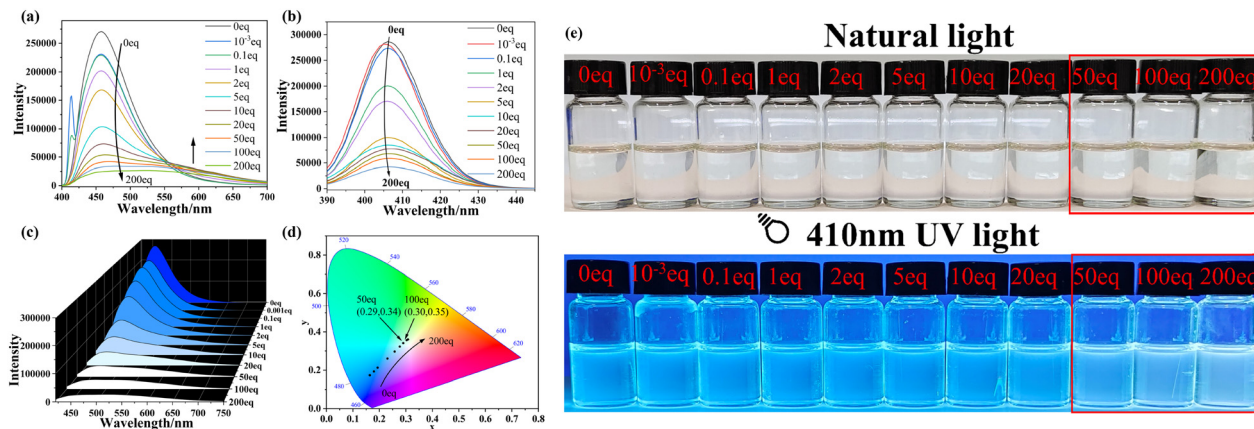


Fig. 3 (a) Fluorescence emission spectroscopy of PI in DMSO solution with increasing concentration of  $H^+$  (0–200 eq.) ( $[PI] = 1 \times 10^{-3} \text{ mol L}^{-1}$ ). (b) Fluorescence absorption spectroscopy of PI in DMSO solution with increasing concentration of  $H^+$  (0–200 eq.) ( $[PI] = 1 \times 10^{-3} \text{ mol L}^{-1}$ ). (c) Fluorescence color change of DMSO solution pertaining to curve (a). (d) CIE gamut diagram corresponding to (a). (e) Color changes of PI in DMSO solution under natural- and UV-light irradiation with increasing  $H^+$  content.

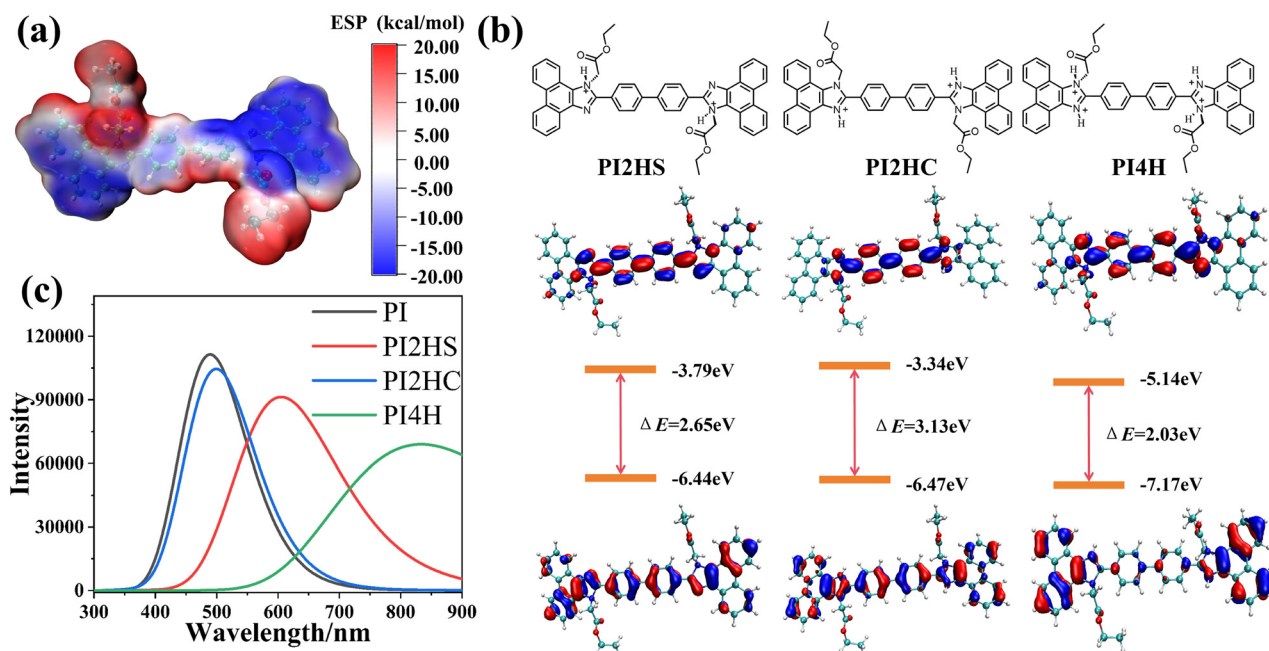


Fig. 4 (a) Simulated electrostatic potential (ESP) distribution of PI. Atomic color codes are C (gray), H (white), O (red), and N (blue). (b) Representation of HOMO–LUMO and energy gap in PI after binding with  $H^+$  at different reaction sites. (c) Fluorescence emission spectra of PI, PI2HS, PI2HC, and PI4H molecules using Gaussian 09.

interactions between PI and  $H^+$  in DMSO solution (Fig. 4b). Based on this simulation, the frontier molecular orbitals of the protonated compound and resulting fluorescence emission spectrum were plotted. Fig. 4b shows the frontier molecular orbitals of the protonated compound of PI. The fluorescence emission peaks of the protonated compounds of PI show varying degrees of red shift (Fig. 4c), similar to previous results regarding the red shifting of the emission peaks of PI with increasing hydrogen-ion concentration. All these characterization results indicate that as  $H^+$  were added to the DMSO solution of PI,  $H^+$  form protonated compounds with varying

degrees of binding with PI. When these protonated products of PI are mixed in the same system, they precisely form a colored light band from blue to red, and when these lights are mixed together, the PI + 100 eq.  $H^+$  system emits white light (Fig. S11, ESI<sup>†</sup>).

### 3.2. Single-molecule white emission triggered by base

After investigating the reasons behind the acid-induced white-light emission from PI, we assessed the corresponding relationship underlying alkali-induced white-light emission from PI (Fig. 5a and b). In a hydroxide-ion concentration range of

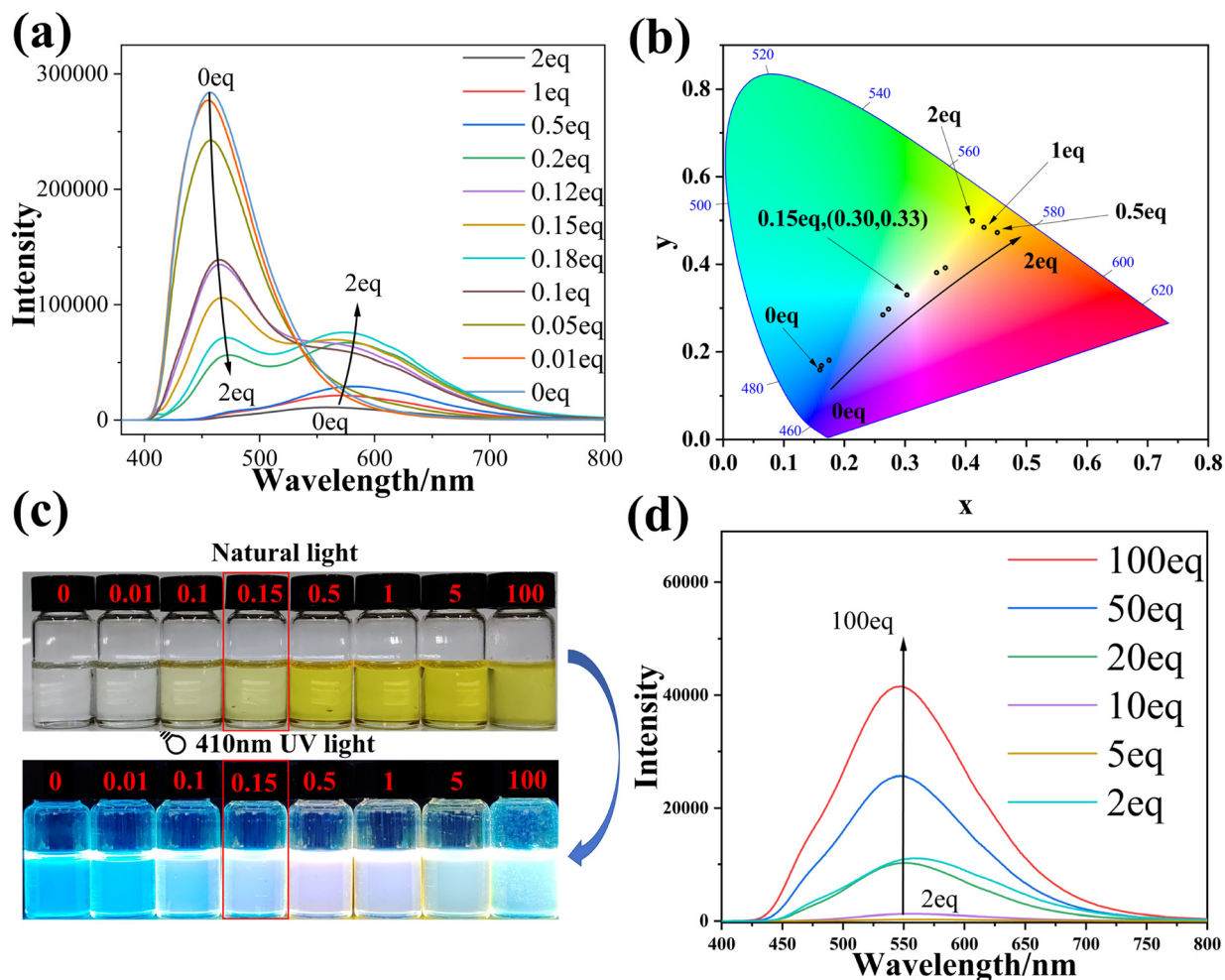


Fig. 5 (a) Fluorescence spectra of PI DMSO solution under increasing OH<sup>-</sup> concentration (0–2 eq.) ([PI] =  $1 \times 10^{-3}$  mol L<sup>-1</sup>). (b) CIE gamut diagram corresponding to (a). (c) Color changes in the PI DMSO solution under natural and ultraviolet light irradiation with increasing OH<sup>-</sup> concentration. (d) Fluorescence spectra of PI DMSO solution under increasing OH<sup>-</sup> concentration (5–100 eq.) ([PI] =  $1 \times 10^{-3}$  mol L<sup>-1</sup>).

0–2 eq., as the hydroxide-ion concentration increased, the fluorescence intensity of the DMSO solution of PI at 458 nm gradually decreased and that at 575 nm gradually increased. When the hydroxide-ion concentration reached 0.15 eq., the DMSO solution of PI exhibited white-light fluorescence emission. The continued increase in the hydroxide-ion concentration caused the fluorescence emission to shift toward yellow fluorescence. When the hydroxide-ion concentration reached 5 eq., the fluorescence emission peaks at 458 and 575 nm disappeared and a new fluorescence emission peak emerged at 548 nm. The fluorescence emission peak at 548 nm gradually intensified with increasing hydroxide-ion concentration (Fig. 5d). In addition, the fluorescence color of PI gradually changed from yellow to yellow–green (Fig. S12, ESI<sup>†</sup>). Based on the fluorescence emission spectra shown in Fig. 5a and d, we speculate that as OH<sup>-</sup> ions are added to the DMSO solution of PI, PI and OH<sup>-</sup> in the solution interact with each other. When a small amount of OH<sup>-</sup> ions is added to the DMSO solution of PI, some PI in the solution interacts with OH<sup>-</sup> and emits red light, causing the blue and red light components in

the system fluorescence to complement each other and emit white light. When a large amount of OH<sup>-</sup> ions is added to the DMSO solution of PI, the free PI in the system almost completely disappears, the blue light component of the system disappears, and the system emits yellow–green light (Fig. 5c and Fig. S11, S12, ESI<sup>†</sup>). Unfortunately, the white light emitted by the DMSO solution of PI + 0.15 eq. OH<sup>-</sup> is not stable, which limits the practical application of the system. This is because OH<sup>-</sup> reacts with the ester bond of PI, leading to the consumption of OH<sup>-</sup> in the DMSO solution of PI + 0.15 eq. OH<sup>-</sup> and causing the system to change from white light to blue light (Fig. S13, ESI<sup>†</sup>).

Similarly, we used <sup>1</sup>H NMR to study the effect of OH<sup>-</sup> on PI in DMSO solvent. When 0.5–1 eq. of OH<sup>-</sup> were added to a DMSO-d<sub>6</sub> solution of PI, the gradual addition of DMSO solution of sodium hydroxide to the DMSO-d<sub>6</sub> solution of PI resulted in the progressive shielding of all signals, except those of the methylene and ester groups (Fig. S14, ESI<sup>†</sup>). However, when 5–100 eq. of OH<sup>-</sup> were added to a DMSO-d<sub>6</sub> solution of PI, the PI in the system was almost completely bound with OH<sup>-</sup>.

At this point, the rotation of the benzene ring adjacent to the phenanthroimidazole ring was restricted, which caused the benzene ring to conjugate with the phenanthroimidazole ring, causing a strong deshielding effect on the  $H_a$  on the benzene ring and increasing its chemical shift from 8.18 ppm to 8.39 ppm. In addition, binding of PI with  $OH^-$  weakened the deshielding effect of  $H_b$  on the phenanthroimidazole ring, increasing its chemical shift from 7.90 ppm to 8.00 ppm (Fig. S15, ESI $^\dagger$ ).

To further support our hypothesis based on the fluorescence spectroscopy results that the DMSO solution of PI was affected by  $OH^-$ , we used FT-IR to elucidate interactions between the aromatic ring of PI and  $OH^-$  after the addition of 0.15 and 100 eq. of  $OH^-$ . The out-of-plane bending vibration of the C-H bond on the aromatic ring of PI in DMSO solution was detected at  $956\text{ cm}^{-1}$  (Fig. S10, ESI $^\dagger$ ). However, after adding 0.15 and 100 eq. of  $OH^-$ , this peak was blue shifted by 3–28  $\text{cm}^{-1}$  (PI + 0.15 eq.  $OH^-$ :  $959\text{ cm}^{-1}$ ; PI + 100 eq.  $OH^-$ :  $984\text{ cm}^{-1}$ ), which to some extent proved the interaction between PI and  $OH^-$ .

### 3.3. Writing gel material for information encryption

Based on the above phenomenon, we further introduced the PI molecules into polymer gel and film and developed a new information-encryption system. The PVA/PI + 100 eq.  $H^+$  gel was prepared by adding PVA to a DMSO solution of PI + 100 eq.  $H^+$ , followed by heating, dissolution and cooling processes (Fig. 6a). This PVA gel can suffer a pH adjustment and formed a white-emission gel through pH regulation. In this gel, the polymer network restricts the free movement of PI molecules, but the movement of protons is unaffected. Therefore, the PVA/PI + 100 eq.  $H^+$  gel exhibited white fluorescence. When the gel surface is in contact with water, the protonated PI on the gel surface deprotonates, causing green fluorescence on the gel surface. Interestingly, we found that the green fluorescence gradually decreases over time, and disappears completely after 40 minutes (Fig. 6b). This information self-elimination process is attributed to the concentration migration of protons. By utilizing this characteristic, we have developed an advanced material with time-dependent encryption, as shown in Fig. 6c.

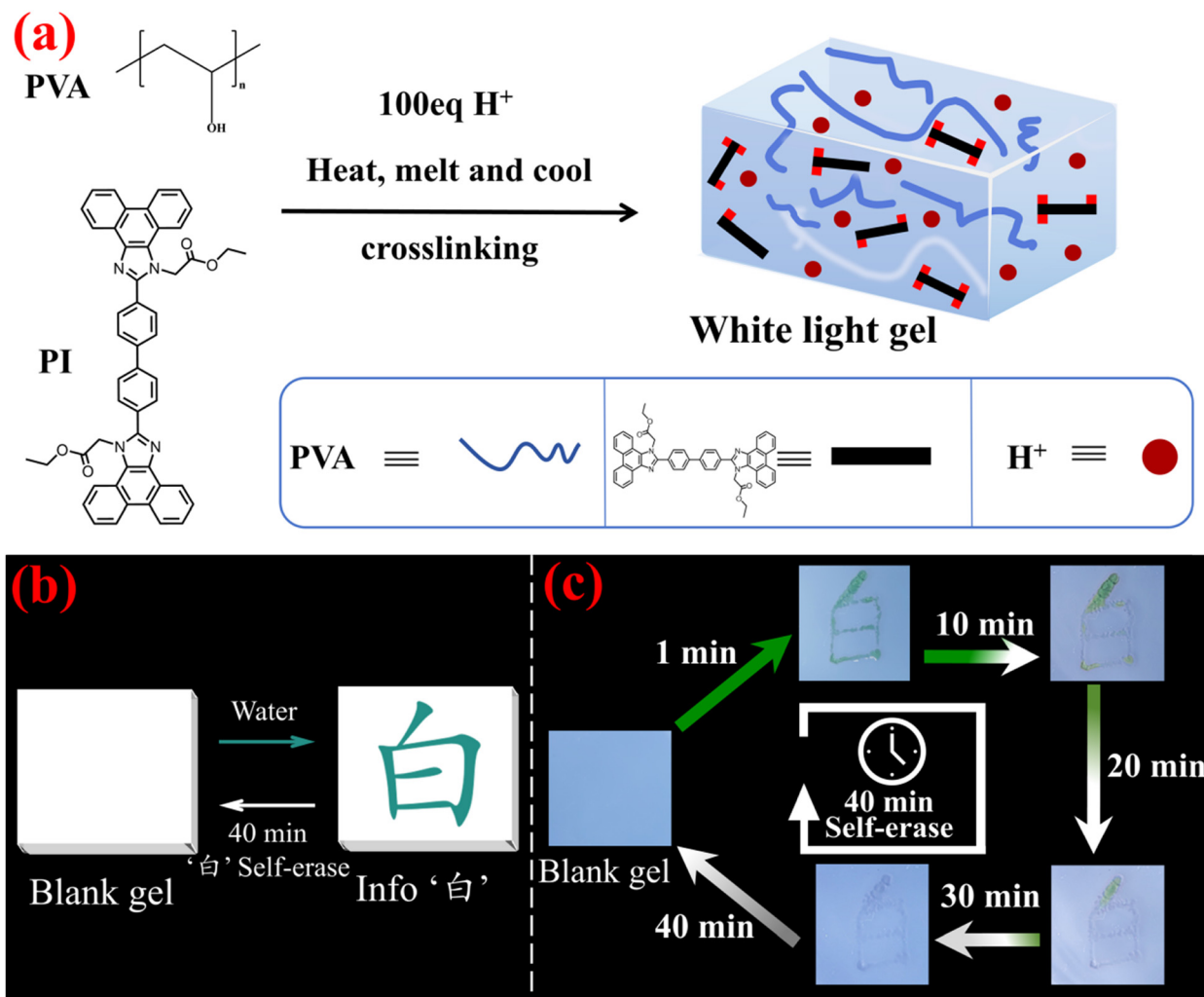


Fig. 6 (a) Schematic of the preparation of the PVA/PI gels. (b) Schematic of information-encoding and self-erasing process of the PVA/(PI + 100 eq.  $H^+$ ) gel. (c) Photograph of PVA/(PI + 100 eq.  $H^+$ ) gel self-erasing process with time under UV light.

When text was inscribed on the PVA/(PI + 100 eq. H<sup>+</sup>) gel surface with distilled water, the fluorescent color at the writing area changed from white light to cyan light. After a certain period, the green fluorescence area on the PVA/(PI + 100 eq. H<sup>+</sup>) gel returned to white light. This was because the concentration of H<sup>+</sup> in the gel was higher than that in the distilled water. This caused H<sup>+</sup> in the gel to diffuse into the distilled water area, deprotonating the protonated PI at the surface of the gel and causing the fluorescence emission of the written characters to change. After a certain period, due to the dynamic network of the gel, missing H<sup>+</sup> at the junction between the gel and water was supplemented, which caused the junction to emit white light again. Thus, the PVA/(PI + 100 eq. H<sup>+</sup>) gel emitting white light can be used as a material for time-dependent information encryption. It is worth mentioning that this self-elimination process is affected by temperature, and the self-elimination time will be shortened to 30 minutes at 60 °C, which is similar to the effect of temperature on the ion migration rate. In addition, these materials exhibit excellent reusability: the erasing process can be repeated more than 15 times (Fig. S16, ESI†).

## 4. Conclusion

A fluorescent molecule PI with the AIE effect was synthesized in this study. Through calculation and experimental characterization, it was confirmed that PI interacts with protons to produce various species, which can individually emit light of different wavelengths. Upon the addition of different amounts of acids, various protonated ionic species are formed, which can emit different colors of light. The mixing of these species caused white emission, leading to single-molecule-based white emission. In addition, the base has a similar effect in producing white emission. Finally, a white-light fluorescent gel was prepared with polyvinyl alcohol as the carrier. The prepared gels could show information upon contact with water vapor, which disappeared after a long time. Thus, a gel-based information-writing and time-dependent information-encryption material was developed.

## Author contributions

Yuehua Liang: conceptualization, methodology, investigation, writing-original draft. Jiuzhi Wei: characterize materials, performance tests. Juan Zhang, Tingting Zhang, Caiyuan Guo and Yanyan Li: performance tests. Xinxian Ma: resources, funding acquisition. Minghua Liu and Yun Yan: writing – review & editing.

## Data availability

The data supporting this article have been included as part of the ESI.†

## Conflicts of interest

There are no conflicts to declare.

## Acknowledgements

This work was supported by the National Natural Science Foundation of China (22462030, 32360327), the Natural Science Foundation of Ningxia, China (2024AAC02050), the Key Laboratory of Green Catalytic Materials and Technology of Ningxia (ZDSYS03), and all of which are gratefully acknowledged.

## Notes and references

- 1 B. Kumari, R. Dahiwadkar and S. Kanvah, *Angew. Chem., Int. Ed.*, 2022, **3**, e191.
- 2 D. Li, J. Wang and X. Ma, *Adv. Opt. Mater.*, 2018, **6**, 1800273.
- 3 D. Das, P. Gopikrishna, D. Barman, R. B. Yathirajula and P. K. Iyer, *Nano Convergence*, 2019, **6**, 31.
- 4 X. Ma, Y. Liang, J. Wei, J. Zhang, E. Feng, Z. Fu, S. Lian and Y. Yan, *ACS Appl. Opt. Mater.*, 2024, **2**, 1903.
- 5 X. Wen, S. Du, L. Zhang and M. Liu, *Angew. Chem., Int. Ed.*, 2023, **62**, e202311816.
- 6 W. Chen, C. Xu, L. kong, X. Liu, X. Zhang, N. Lin and X. Ouyang, *Adv. Opt. Mater.*, 2022, **10**, 2102742.
- 7 Q. Huang, Q. Guo, J. Lan, R. Su, Y. Ran, Y. Yang, Z. Bin and J. You, *Mater. Horiz.*, 2021, **8**, 1499.
- 8 Z. Wei, Y. Zhang and X. Zhang, *Dyes Pigm.*, 2023, **216**, 111347.
- 9 J. Zhang, P. Alam, S. Zhang, H. Shen, L. Hu, H. H. Y. Sung, I. D. Williams, J. Sun, J. W. Y. Lam, H. Zhang and B. Z. Tang, *Nat. Commun.*, 2022, **13**, 3492.
- 10 J. Wang, F. Tang, Y. Wang, S. Liu and L. Li, *Adv. Opt. Mater.*, 2020, **8**, 1901571.
- 11 A. Maity, F. Ali, H. Agarwalla, B. Anothumakkool and A. Das, *Chem. Commun.*, 2015, **51**, 2130.
- 12 T. Antón-Cánovas, S. Achelle, M. Paz Fernández-Lienres, A. Navarro, F. Alonso and J. Rodríguez-López, *J. Mol. Liq.*, 2023, **380**, 121758.
- 13 C. Shang, G. Wang, K. Liu, Q. Jiang, F. Liu, P. T. Chou and Y. Fang, *Angew. Chem., Int. Ed.*, 2020, **59**, 8579.
- 14 K. Imamura, Y. Ueno, S. Akimoto, K. Eda, Y. Du, C. Eerdun, M. Wang, K. Nishinaka and A. Tsuda, *ChemPhotoChem*, 2017, **1**, 427.
- 15 J. Chen, Q. Peng, J. Liu and H. Zeng, *Langmuir*, 2023, **39**, 17600.
- 16 H. Geng, P. Zhang, Q. Peng, J. Cui, J. Hao and H. Zeng, *Acc. Chem. Res.*, 2022, **55**, 1171.
- 17 Y. Wu, R. Wang, R. Lin, X. Xu, X. Zhang, O. Alsalman, Y. Qiu, A. Uddin and X. Ouyang, *Chem. Eng. J.*, 2023, **465**, 142929.
- 18 Y. Wu, R. Lin, M. Iqbal, Y. Jin, Y. Huo and X. Ouyang, *J. Comput. Chem.*, 2022, **10**, 3103–3113.
- 19 Q. Wang, Z. Qi, Q. M. Wang, M. Chen, B. Lin and D. H. Qu, *Adv. Funct. Mater.*, 2022, **32**, 2208865.
- 20 Y. Liu, M. Li, H. Ju, Z. Wang, Y. Wu, Z. L. Wu, H. Zhu and F. Huang, *Polym. Chem.*, 2022, **13**, 6255.
- 21 W. Humphrey, A. Dalke and K. Schulten, *J. Mol. Graphics*, 1996, **14**, 33.
- 22 T. Lu and F. Chen, *J. Comput. Chem.*, 2011, **33**, 580.